Int J Thermophys (2010) 31:710–716
DOI 10.1007/s10765-010-0707-y

Specific Heat Capacity of Nitrobenzene–Tetradecane Near the Liquid–Liquid Critical Point

P. Losada-Perez · G. Cordoyiannis · C. A. Cerdeiriña · C. Glorieux · J. Thoen

Received: 27 June 2009 / Accepted: 17 January 2010 / Published online: 10 February 2010

Abstract High-resolution adiabatic scanning calorimetry has been used to study the specific heat capacity anomaly of the nitrobenzene–tetradecane mixture near its upper critical point. The analysis, which is based on a method that uses heat capacity and enthalpy data, yields a value of the critical amplitude ratio A^+/A^- which is consistent with the universal, accepted one. The critical amplitude of the correlation length was derived via two-scale factor universality. All this information is compared to that reported in previous studies for nitrobenzene–alkane mixtures.

Keywords Adiabatic scanning calorimetry · Binary mixtures · Correlation length · Critical behavior · Isobaric heat capacity

P. Losada-Perez · C. A. Cerdeiriña
Departamento de Física Aplicada, Universidad de Vigo, As Lagoas s/n, 32004 Ourense, Spain

G. Cordoyiannis · C. Glorieux · J. Thoen
Laboratorium voor Akoestiek en Thermische Fysica, Departement Sterrenkunde en Natuurkunde, Katholieke Universiteit Leuven, 3001 Leuven, Belgium

P. Losada-Perez (✉)
Laboratorium voor Akoestiek en Thermische Fysica (ATF), Dep. Fysica en Sterrenkunde, Katholieke Universiteit Leuven, Celestijnenlaan 200D, 3001 Leuven, Belgium
e-mail: patriciamaria.losadaperez@fys.kuleuven.be; patilosada@uvigo.es

Present Address:
G. Cordoyiannis
Condensed Matter Physics Department, Jozef Stefan Institute, Jamova 39, 1000 Ljubljana, Slovennia

1 Introduction

Besides liquid–gas phase transitions, binary mixtures exhibit liquid–liquid separation or demixing, which is characterized by the coexistence of two equilibrium liquid phases of different composition. On the basis of the so-called isomorphism of critical phenomena [1], thermodynamic analogies between liquid–gas and liquid–liquid criticality exist; in other words, within the same universality class (in this particular case, the three-dimensional Ising universality class), the anomalous behavior displayed by analogous thermodynamic properties near liquid–gas and liquid–liquid critical points is characterized by similar power laws. Concretely, the behavior of the specific heat capacity at constant pressure and composition, $C_{p,x}$, of a binary mixture when approaching the liquid–liquid critical point—to which we shall restrict our attention here—finds its analog in the specific heat capacity at constant volume, C_v, of a pure fluid when approaching the liquid–gas critical point.

Along a path of critical composition, the so-called critical isopleth ($x = x_c$), $C_{p,x}$ is known to behave like [2]

$$C_{p,x} = B + ET + A^{\pm} |t|^{-\alpha} \left(1 + D^{\pm} |t|^{\theta} + \cdots\right), \tag{1}$$

where $t \equiv (T - T_c)/T_c$ is the dimensionless temperature critical deviation, $\pm$ refers to the one-phase and two-phase regions ($t > 0$ and $t < 0$, respectively, for an upper consolute point), $\alpha = 0.109 \pm 0.004$ is the critical exponent of the specific heat, $\theta = 0.53 \pm 0.02$ is the leading correction-to-scaling critical exponent [3], and $A^{\pm}$ and $D^{\pm}$ are (system-dependent) critical amplitudes.

The validity of Eq. 1 has been checked for a wide variety of binary mixtures via the experimental determination of α and some universal relations involving $A^{\pm}$ [4]. Nevertheless, some specific liquid–liquid systems are problematic because their $A^{\pm}$ values are extremely small: two examples are Coulombic ionic solutions [5] and polymer solutions [6]. It is therefore interesting to test how sensitive current experimental methods for determining $A^{\pm}$ can be. To this end, we have selected the nitrobenzene–tetradecane (NB–$C_{14}H_{30}$) mixture, which, on the basis of previously reported values for other systems of the NB–alkane series [7,8], is expected to exhibit a small critical anomaly. Here, we present results on the $C_{p,x}$ anomaly for this mixture as determined using high-resolution adiabatic scanning calorimetry (ASC), a technique that yields simultaneously the temperature profiles of both the specific heat and the enthalpy, i.e., $C_{p,x}(T)$ and $H(T)$ [9,10].

In particular, we have studied the slope of the chord joining the point (T, H) with the critical point (T_c, H_c) in the $H(T)$ curve. This quantity, to be denoted by C, thus reads

$$C = \frac{H - H_c}{T - T_c}. \tag{2}$$

As we shall see later, C has essentially the same critical behavior as $C_{p,x}$. The advantage of using the former resides in that it considers the chord and not the local derivative, and is thereby less sensitive to noise, thus yielding information of higher quality.

This method was successfully checked in the past [11] for triethylamine–water, which displays a remarkably high critical anomaly in the specific heat.

From $A^{\pm}$ values, we derived the ratio A^{+}/A^{-} and, using two-scale factor universality, the critical amplitude of the correlation length ξ_0^{+}. The consistency of the results thus determined is tested against all available information on these quantities. The manuscript is organized as follows. In Sect. 2, information regarding the samples and the mixture preparation as well as the experimental technique is given. A detailed explanation of data treatment is presented in Sect. 3. Afterwards, the results are discussed in Sect. 4 and, finally, conclusions are provided in Sect. 5.

2 Samples and Apparatus

The compounds used for this work have been purchased from Fluka. Nitrobenzene is of assay >99.5 % (mass percent by gas chromatography), while tetradecane is of assay >99.5 % (mass percent by gas chromatography) and it is reported to be olefin-free. Both chemicals were used without further purification, and the mixture preparation was done under a nitrogen atmosphere. Both the cell and the sample were weighed using a Mettler-Toledo XS204 balance; the uncertainty in the NB mole fraction x was about 0.001.

The calorimeter is computer-controlled, and it consists of four stages, the first (inner) one comprise the sample and the cell and three surrounding shields. The space between the various stages is vacuum-pumped to achieve maximum thermal insulation. The extremely slow scanning rates that can be achieved with ASC reveal highly precise H, $C_{p,x}$, and C data. More details can be found in [11].

For the actual experiment, we have used a cylindrical 54-g tantalum cell that contained 10.9 g of sample at the critical concentration (x_c). As a guide for x_c, we used the data of An et al. [12] as well as measurements on the dielectric constant [13], which yield $x_c = 0.678 \pm 0.001$. To get good temperature control in such a rather large sample, stirring was performed throughout the experiment. This could be achieved by inserting a stainless steel ball in the cylindrical cell. Then, by changing the inclination of the whole apparatus (via an automatic hydraulic mechanism), the ball was moving back and forth inside the cell. In addition, the heat capacity of the empty cell was measured in a separate experiment and it was subtracted from the total heat capacity (sample plus cell) to obtain the net $C_{p,x}$ of the NB–$C_{14}H_{30}$ critical mixture. Furthermore, the temperature profile of $H(T)$ was measured upon slowly cooling the sample with a (small) scanning rate of $20\,\mathrm{mK}\cdot\mathrm{h}^{-1}$. Upon cooling, a negative power is applied to the sample cell. This can be achieved by creating a constant temperature difference between the sample and first shield, i.e., the shield is kept at a lower temperature than the cell, resulting in a constant negative leak power [10].

3 Methodology for Data Treatment

The underlying theoretical background to our analysis starts from Eqs. 1 and 2 in Sect. 1. Hence, the enthalpy in the one-phase region can be expressed as

$$H = H_s + \int_{T_s}^{T} C_p \mathrm{d}T, \tag{3}$$

where H_s and T_s denote the starting values of enthalpy and temperature, respectively. By substituting Eq. 1 in Eq. 3, one obtains

$$H = H_s + \frac{T_c A^+}{1-\alpha}\left[\left(\frac{T-T_c}{T_c}\right)^{1-\alpha} - \left(\frac{T_s-T_c}{T_c}\right)^{1-\alpha}\right] + B(T-T_s) + \frac{E}{2}(T^2 - T_s^2). \tag{4}$$

The critical enthalpy, H_c, is obtained by setting $T = T_c$ in Eq. 4, yielding

$$H_c = H_s - \frac{T_c A^+}{1-\alpha}\left(\frac{T_s-T_c}{T_c}\right)^{1-\alpha} + B(T_c - T_s) + \frac{E}{2}(T_c^2 - T_s^2). \tag{5}$$

By combining Eqs. 4 and 5, one obtains

$$H - H_c = \frac{T_c A^+}{1-\alpha}\left(\frac{T-T_c}{T_c}\right)^{1-\alpha} + B(T-T_c) + \frac{E}{2}(T-T_c)(T+T_c). \tag{6}$$

Finally, by inserting Eq. 6 into Eq. 2, the following explicit expression for C is found:

$$C = B' + E'T + A^{+\prime}|t|^{-\alpha}, \tag{7}$$

where

$$A^{+\prime} = \frac{A^+}{1-\alpha}, \quad B' = B + \frac{ET_c}{2}, \quad E' = \frac{E}{2}. \tag{8}$$

By comparing Eqs. 1 and 7, one concludes that the critical behavior of C is essentially the same as that of $C_{p,x}$, but with coefficients renormalized as shown in Eq. 8. In particular, the critical amplitude is enlarged by a factor $(1-\alpha)^{-1}$. Proceeding in the same way, corresponding expressions for the two-phase region are easily obtained.

4 Results and Discussion

In Fig. 1, the experimental C data are presented for the range $|t| < 10^{-3}$. The solid lines in this figure correspond to a fitting result with Eq. 7. The T_c and corresponding H_c values were derived from the direct experimental $H(T)$ results. The optimal value obtained for T_c was 305.0260 K with an uncertainty of 0.5 mK. The corresponding changes in H_c were $\pm 1\,\mathrm{J\cdot kg^{-1}}$. Fits with Eq. 7 and with $\alpha = 0.109$ were initially carried out with linear and quadratic terms in the background. It turned out that, given the

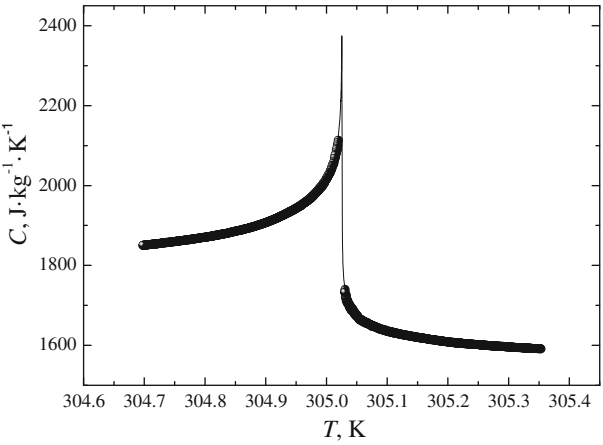

Fig. 1 Temperature profile of the quantity C. *Symbols* are experimental data, while the *solid line* corresponds to the fitted values to Eq. 7 and its two-phase region counterpart. Data points within $|t| < 10^{-4.5}$ have been excluded, since there is rounding for ±5 mK around T_c for the scanning rate chosen

small working temperature interval ($|t| < 10^{-3}$), the constant term in Eq. 7 was sufficient to achieve high-quality fits. Fits with additional terms in the background resulted in equally good fits, but with strong parameter correlations. The fitting curves in Fig. 1 are calculated with the following parameters: $B' = (1339 \pm 14)\,\mathrm{J \cdot kg^{-1} \cdot K^{-1}}$, $A^{+\prime} = (120 \pm 6)\,\mathrm{J \cdot kg^{-1} \cdot K^{-1}}$, $A^{-\prime}=(243 \pm 5)\,\mathrm{J \cdot kg^{-1} \cdot K^{-1}}$, and $T_c=(305.0260 \pm 0.0005)$ K. The uncertainties in the other parameters reflect the uncertainty in the quoted T_c value. Correction-to-scaling terms have not been included in the fitting equation because of the small $|t|$ range considered. Including the first-order correction term in the fitting did not improve the quality of the fits. A log $(C - B')$ versus log$|t|$ plot is depicted in Fig. 2, where experimental data are compared with straight lines with a fixed slope of −0.109. The values of the $C_{p,x}$ amplitude counterparts can be easily obtained by means of the relations given by Eq. 8. This results in $B = (1339 \pm 14)\,\mathrm{J \cdot kg^{-1} \cdot K^{-1}}$, $A^{+\prime} = (107 \pm 5)\,\mathrm{J \cdot kg^{-1} \cdot K^{-1}}$, and $A^{-\prime} = (216 \pm 4)\,\mathrm{J \cdot kg^{-1} \cdot K^{-1}}$.

The A^+/A^- ratio equals that of $A^{+\prime}/A^{-\prime}$, as follows from Eq. 8. From the above values, we find $A^+/A^- = 0.49 \pm 0.03$, which is in agreement with the theoretical value of 0.53 ± 0.02 [4]. From $A^{+\prime}$, we also estimate the critical amplitude of the correlation length via two-scale factor universality. This theoretical result establishes that the quantity $X = \alpha A_v^+ \xi_0^{+3}/k_B$, where A_v denotes the critical amplitude of the specific heat per unit volume and k_B represents the Boltzmann constant, which is universal, with its theoretical value being 0.0190 ± 0.004 [4]. Thus, $A^{+\prime}$ has been converted to A_v^+ via $A_v^+ = (1 - \alpha)A^{+\prime}V_c$, where V_c is the critical volume per kg of the mixture (which has been estimated assuming ideal volumetric mixing), to obtain $A_v^+ \approx (0.011 \pm 0.003)\,\mathrm{J \cdot cm^{-3} \cdot K^{-1}}$ and $\xi_0^+ = (0.286 \pm 0.019)$ nm.

Figure 3 shows the trends of both (a) A_V^+ and (b) the predicted ξ_0^+ values for various systems of the NB–C_NH_{2N+2} (where N denotes the number of carbon atoms of the alkane) series. For ξ_0^+, values obtained from turbidity measurements by Zhou et al. [14] and Beysens et al. [15] as well as those determined from ellipsometry [16] and

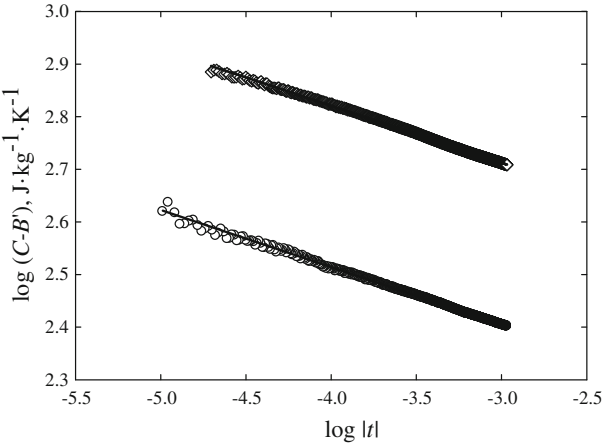

Fig. 2 Log $(C - B')$ versus log $|t|$ plot. *Circles* represent values in the one-phase phase region, *diamonds* represent values in the two-phase region, and *solid lines* represent straight lines with the slope fixed to the theoretical value $-\alpha = -0.109$

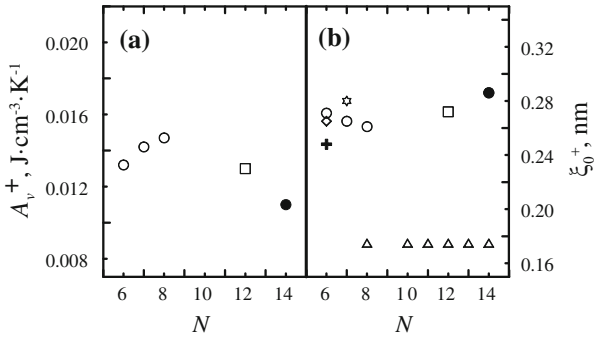

Fig. 3 Critical amplitudes of (**a**) the specific heat capacity per unit volume A_v^+ and (**b**) the correlation length ξ_0^+ for NB–$C_N H_{2N+2}$ critical mixtures. *Open circles* [5], *open squares* [6], *black circles* this work, *open triangles* [11], *open diamonds* [12], *stars* [13], and *crosses* [14]

X-ray scattering [17] are also represented in (b). As can be observed, A_v^+ hardly varies with N; indeed, our A_v^+ value for $N = 14$ is consistent with the trend inferred from the behavior of mixtures with lower alkanes [7,8]. As regards ξ_0^+, there exists a significant discrepancy between the values obtained from calorimetry and those derived from the turbidity measurements by Zhou et al. [14]. Conversely, as noticed previously [7], values for $N = 6$ and $N = 7$ determined from turbidity experiments by Beysens et al. compare favorably with those obtained from calorimetry, ellipsometry, and X-ray scattering.

5 Conclusion

By studying the critical behavior of the quantity $C(T)$ for nitrobenzene–tetradecane, we have extended the previous analysis for triethylamine–water to a new binary

mixture. From comparisons with literature data for nitrobenzene–alkane critical mixtures, it is concluded that the method is fairly efficient for the actual system, which, we recall, is characterized by a rather small critical anomaly. We may assert that the study of $C(T)$ using ASC should be regarded as a promising approach to the determination of extremely small critical amplitudes in liquid–liquid criticality.

Acknowledgments This research was supported by the "Ministerio de Educación y Ciencia" under the "Programa Nacional de Formación del Profesorado Universitario," with assistance to P. Losada-Pérez (#AP-2004-2947 grant). Assistance to George Cordoyiannis was supported by a postdoctoral grant by the FWO (Flanders research foundation).

References

1. M.A. Anisimov, E.E. Gorodetskii, V.D. Kulikov, J.V. Sengers, Phys. Rev. E **51**, 1199 (1995)
2. A. Kumar, H.R. Krishnamurthy, E.S.R. Gopal, Phys. Rep. **98**, 57 (1983)
3. M. Barmatz, I. Hahn, J.A. Lipa, Rev. Mod. Phys. **79**, 1 (2007)
4. V. Privman, P.C. Hohenberg, A.A. Aharony, in *Phase Transitions and Critical Phenomena*, vol. 14, ed. by C. Domb, J.L. Lebowitz (Academic Press, New York, 1991)
5. T. Heimburg, S.Z. Mirzaev, U. Kaatze, Phys. Rev. E **62**, 4963 (2000)
6. M.A. Anisimov, A.F. Kostko, J.V. Sengers, Phys. Rev. E **165**, 051805 (2002)
7. M. Souto-Caride, J. Troncoso, E. Carballo, L. Romaní, Chem. Phys. **324**, 483 (2006)
8. N.J. Utt, S.Y. Lehman, D.T. Jacobs, J. Chem. Phys. **127**, 104505 (2007)
9. J. Thoen, E. Bloemen, H. Marynissen, W. Van Dael, in *Proceedings of the 8th Symposium on Thermophysical Properties*, National Bureau of Standards, Gaithersburg, MD, 1981 (ASME, New York, 1982), pp. 422–428
10. J. Thoen, in *Heat Capacities: Liquids, Solutions and Vapours*, ed. by E. Whilhem, T.M. Letcher (The Royal Society of Chemistry, London, 2010), chap. 13, pp. 287-306
11. E. Bloemen, J. Thoen, W. Van Dael, J. Chem. Phys. **73**, 4628 (1982)
12. X. An, H. Zhao, F. Jiang, C. Mao, W. Shen, J. Chem. Thermodyn. **29**, 1047 (1997)
13. J. Leys, P. Losada-Perez, G. Cordoyiannis, C.A. Cerdeirina, C. Glorieux, J. Thoen, J. Chem. Phys. (in press)
14. C. Zhou, X. An, F. Jiang, H. Zhao, W. Shen, J. Chem. Thermodyn. **31**, 615 (1999)
15. D. Beysens, A. Bourgou, G. Paladin, Phys. Rev. A **30**, 5 (1984)
16. A. Hirtz, W. Lawnik, G.H. Findenegg, Colloids Surf. **51**, 405 (1990)
17. E.M. Dufresne, T. Nurushev, R. Clarke, S. Dierker, Phys. Rev. E **65**, 061507 (2002)